Clinical Biochemistry 44 (2011) 975–979

Contents lists available at ScienceDirect

Clinical Biochemistry

journal homepage: www.elsevier.com/locate/clinbiochem

Impact of contrast enhanced MRI on lymphocyte DNA damage and serum visfatin level

Sema Yildiz [a,*], Hasan Cece [a], Ihsan Kaya [a], Hakim Celik [b], Abdullah Taskin [b], Nurten Aksoy [b], Abdurrahim Kocyigit [b], Mehmet A. Eren [c]

[a] Harran University School of Medicine, Department of Radiology, 63100, Sanliurfa, Turkey
[b] Harran University School of Medicine, Department of Clinical Biochemistry, 63100, Sanliurfa, Turkey
[c] Harran University School of Medicine, Department of Internal Medicine, 63100, Sanliurfa, Turkey

ARTICLE INFO

Article history:
Received 19 March 2011
Received in revised form 6 May 2011
Accepted 7 May 2011
Available online 18 May 2011

Keywords:
Alkaline comet assay
Gadolinium based contrast agents
High sensitive C reactive protein
Lymphocyte DNA damage
Magnetic resonance imaging
Nephrogenic systemic fibrosis
Visfatin

ABSTRACT

Objectives: Nephrogenic systemic fibrosis is a novel clinical entity encountered in subjects undergoing contrast enhanced magnetic resonance imaging (MRI). The aim of the present study is to evaluate the impact of contrast enhanced MRI exposure on lymphocyte DNA damage and serum levels of visfatin.
Design and methods: Twenty-eight subjects undergoing contrast enhanced hypophysial MRI with omniscan® were included in the study. Blood samples were drawn before MRI, after non-contrast MRI and after contrast enhanced MRI from each subject. Lymphocyte DNA damage was analyzed by the alkaline comet assay, whereas serum visfatin level was assessed with enzyme immuno assay.
Results: Both lymphocyte DNA damage and serum visfatin levels were statistically significantly increased in samples withdrawn after contrast enhanced MRI compared to samples withdrawn after non-contrast enhanced MRI and baseline samples (ANOVA $p<0.001$, for both).
Conclusions: Findings of the present study revealed that the contrast enhanced MRI is associated with increased lymphocyte DNA damage and increased serum visfatin level.

Introduction

Nephrogenic systemic fibrosis (NSF) is a well-known clinical entity first described in the medical literature in 2000 [1] and is characterized with cutaneous hyperpigmentation, indurations and joint contractures. Histopathologic features of NSF have either been defined as fibroplastic lesions characterized with irregularly arranged dermal collagen bundles with surrounding clefts and a strikingly increased number of similarly arranged spindled and plump fibroblast-like cells with a concomitant increase in interfibrillar mucin [1–4], likened to scleroderma, or as florid fibroplasia, resembling the cellular phase of acute wound healing [5]. Dense, thickened collagen bundles besides increase in collagen, hyaluronan, matrix proteins and inflammatory and profibrotic cytokines have also been reported in NSF [6].

The mechanistic events that lead from gadolinium-based contrast agents (GBCA) exposure to NSF are yet to be fully established although undergoing contrast enhanced magnetic resonance imaging (MRI) was reported to increase incidence of NSF especially in the presence of renal insufficiency [1,2,7,8]. Decreased GBCA clearance or several other deficits that predispose to fibroplasia and fibrosis in individuals with kidney disease might be mechanism (s) linking NSF and renal insufficiency.

Peripheral lymphocyte DNA damage, assessed with Comet assay, is a well-established method to reveal DNA strand breaks due to several mechanisms [9]. Visfatin is a proinflammatory adipocytokine that is produced by various tissues, including skeletal muscle, liver, and bone marrow, and by immune cells such as neutrophil and lymphocyte [10] and induces production of several inflammatory cytokines [11], whereas high sensitive C-reactive protein (hsCRP) is a well-known surrogate marker of inflammation secreted in response to several proinflammatory cytokines.

We hypothesized that the contrast enhanced MRI would induce lymphocyte DNA damage and would increase serum levels of inflammatory/proinflammatory markers. Accordingly, this study was mainly planned to evaluate the association between contrast enhanced MRI exposure and lymphocyte DNA damage besides serum levels of visfatin and hsCRP in subjects undergoing contrast enhanced hypophysial MRI.

Abbreviations: ANOVA, analysis of variance; DNA, deoxyribonucleic acid; EDTA, ethylenediaminetetraacetic acid; GBCA, gadolinium based contrast agent; HDL, high density lipoprotein; hsCRP, high sensitive C reactive protein; LDL, low density lipoprotein; MMP, matrix metalloproteinase; MRI, magnetic resonance imaging; NSF, nephrogenic systemic fibrosis; PBS, phosphate buffered saline; TIMP, tissue inhibitor of metalloproteinase; VEGF, vascular endothelial growth factor; VLDL, very low density lipoprotein.

* Corresponding author. Fax: +90 414 315 11 81.
E-mail address: drsemayildiz@yahoo.com (S. Yildiz).

0009-9120/$ – see front matter © 2011 The Canadian Society of Clinical Chemists. Published by Elsevier Inc. All rights reserved.
doi:10.1016/j.clinbiochem.2011.05.005

Materials and methods

Study population

The study was consisted of 28 subjects undergoing contrast enhanced hypophysial MRI. All subjects were from the same geographical region and had a similar dietary pattern. Study protocol conforms to the principles outlined in Declaration of Helsinki and was approved by institutional ethics review board and informed consent for participation was obtained.

Exclusion criteria were the presence of neoplastic diseases, inflammatory diseases such as infections and autoimmune disorders, cardiovascular, liver and kidney diseases, hypertension, diabetes, recent major surgical procedure (s); use of antioxidant drugs such as statins and vitamins E and C, alcohol use and smoking.

Contrast enhanced magnetic resonance imaging

The MRI examinations were performed on 1.5 Tesla superconducting system (Magnetom Symphony®, Siemens, Erlangen, Germany) with a maximum gradient field strength of 30 mT/m, slew rate 125 T/m/s, and a minimum gradient rise time of 240 microsecond using a standard 12 channel head coil at standard 22 °C temperature. Intravenous GBCA (Omniscan®, Amersham Health, Oslo, Norway) was rapidly injected (2 mL/sec) at a dosage of 0.1 mmol/kg body weight for performing contrast enhanced MRI. Standard turbo spin echo, and spin echo pulse sequences were utilized to generate non-contrast enhanced and contrast enhanced images listed in Table 1.

Blood sampling protocol

Peripheral venous blood samples were drawn into heparinized tubes in the fasting state for three times in each subject: First just before the MRI examination, second after non-contrast enhanced T1 and T2 weighted scans, and third at the end of the contrast enhanced MRI examination.

One milliliter of each venous blood sample was immediately pipetted into another tube to measure DNA damage. The remaining blood was centrifuged at 3000 rpm for 10 min for plasma separation. Samples were stored at −80 °C until analyses for levels of visfatin, hsCRP, urea, creatinine, uric acid, fasting glucose, triglyceride, total cholesterol, high density lipoprotein (HDL) cholesterol, low density lipoprotein (LDL) cholesterol, and very low density lipoprotein (VLDL) cholesterol.

Table 1
Non-contrast enhanced and contrast enhanced Magnetic Resonance Images.

Image	Estimated mean duration
Non-contrast enhanced	
1-Localizer	10sec[a]
2-T2-weighted TSE[b]:coronal, TR[c] = 3500ms[d], TE[e] = 110 ms	2min[f] 11 sec
3-T1-weighted SE[g] coronal, TR = 494 ms, TE = 11 ms	3 min 24 sec
4-T1-weighted TSE sagittal, TR = 494 ms, TE = 11 ms	2 min 24 sec
Contrast enhanced	
5-T1-weighted TSE coronal dynamic scan TR = 100 ms, TE = 3.67 ms	1 min 55 sec
6-T1- weighted SE sagittal FAT-SAT[h] TR = 400 ms, TE = 8.7 ms	2 min 45 sec
7-T1- weighted SE coronal FAT-SAT TR = 494 ms, TE = 11 ms	3 min 24 sec

Abbreviations: [a]sec: seconds, [b]TSE: turbo spin echo, [c]TR: time of repetition, [d]ms: milliseconds, [e]TE: time of echo, [f]min: minutes, [g]SE: spin echo, [h]FAT-SAT: fat saturation.

Determination of lymphocyte DNA damage by the alkaline comet assay

Lymphocyte isolation for the comet assay was performed by density gradient separation (Histopaque 1077, Sigma-Aldrich®, St. Louis, MO, USA). Heparinized blood of 1 mL was carefully layered over 1 mL Histopaque and centrifuged for 35 min at 500 ×*g* and at 25 °C. The interface band containing lymphocytes was washed with phosphate-buffered saline (PBS) and then collected by 15 min centrifugation at 400 ×*g*. The resulting pellets were resuspended in PBS to obtain 20,000 cells in 10 μl. Membrane integrity was assessed by trypan blue exclusion.

Endogenous DNA damage in lymphocytes was analyzed by the alkaline comet assay as described by Singh et al. [12] with minor modifications. Fresh lymphocyte cell suspension of 10 μl (about 20,000 cells) was mixed with 80 μl of 0.7% low-melting point agarose (LMPA) (Sigma) in PBS at 37 °C. Subsequently, 80 μl of this mixture was layered onto slides that had previously been coated with 1.0% hot (60 °C) normal-melting point agarose (NMPA) and the slides were covered with a coverslip at 4 °C for at least 5 min to allow the agarose to solidify. After removing the coverslips, the slides were submersed in freshly prepared cold (4 °C) lysing solution (2.5 M NaCl, 100 mM EDTA-2Na; 10 mM Tris–HCl, pH 10–10.5; 1% Triton X-100 and 10% DMSO were added just before use) for at least 1 h. The slides were then immersed in freshly prepared alkaline electrophoresis buffer (0.3 mol/l NaOH and 1 mmol/l Na_2ETDA, pH>13) at 4 °C for unwinding (40 min) and then electrophoresed (25 V/300 mA, 25 min). All these steps were conducted under red light or without direct light in order to prevent additional DNA damage. After electrophoresis, the slides were stained with ethidium bromide (2 μ/mL in distilled H_2O; 70 μl/slide), covered with a coverslip, and analyzed using a epifluorescence microscope (Nikon®, Japan) equipped with rhodamine filter (excitation wavelength 546 nm, barrier filter 580 nm). The images of 100 randomly chosen nuclei (50 cells from each of two replicate slides) were analyzed visually. Each image was classified according to the intensity of the fluorescence in the comet tail, which was rated from 0 (from undamaged) to 4 (maximally damaged) (Fig. 1), so that the total score of two replicate slides could be between 0 and 400 arbitrary units. All procedures were performed by the same biochemistry staff and DNA damage was assessed by a single observer who was not aware of samples.

Measurement of serum C-terminal visfatin level

Plasma C-terminal Visfatin levels were determined with Enzyme Immuno Assay by using commercially available kits (Catalogue No. EK-003-80, Phoenix Pharmaceuticals®, CA, USA) with intra- and interassay coefficients of variance of <5% and <14%, respectively. The results were expressed as ng/mL (range: 0.1–1000 ng/mL).

Measurement of other biochemical markers

The levels of hsCRP, urea, creatinine, uric acid, fasting glucose, triglyceride, total cholesterol, HDL-cholesterol, LDL-cholesterol and VLDL-cholesterol were determined using commercially available assay kits (Abbott Aeroset®, Abbott Diagnostics, Abbott Park, IL, USA) with Abbott Aeroset auto-analyzer (Abbott®, IL, USA).

Statistical analysis

Data were analyzed using SPSS (Statistical Package for the Social Sciences, version 11.5 for Windows, SPSS® Inc, Chicago, IL). The results were presented as mean ± standard deviation or frequency. Distribution of parametric variables was assessed with one-sample Kolmogorov–Smirnov test and all parametric variables were found to be normally distributed. Comparison among

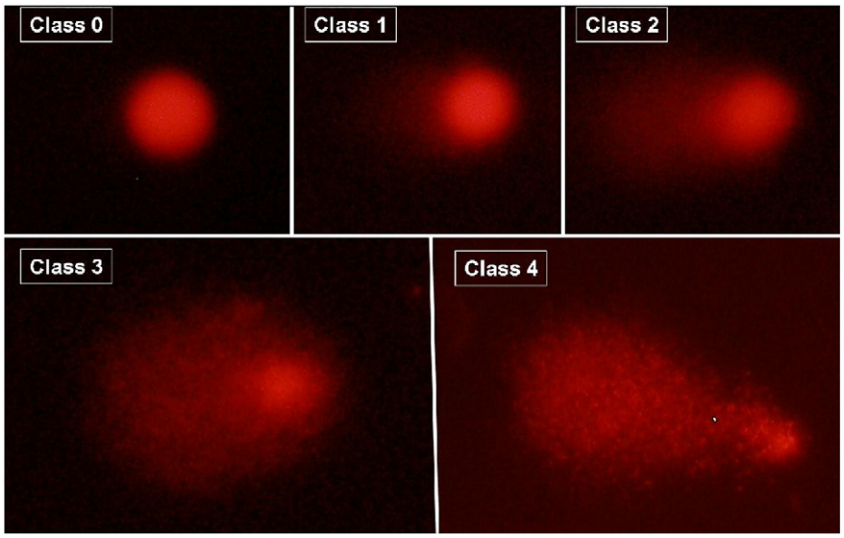

Fig. 1. Photomicrographs showing different images of comet classes (class 0, undamaged; class 4, maximally damaged).

repeated laboratory variables was performed by repeated measures analysis of variance (ANOVA) with Bonferroni post-hoc test. A two-tailed *p* value of less than 0.05 was considered statistically significant.

Results

Baseline demographic and laboratory characteristics of the study population were summarized in Table 2. Lymphocyte DNA damage was statistically significantly increased in samples withdrawn after contrast enhanced MRI compared to baseline samples and compared to samples withdrawn after non-contrast enhanced MRI (Fig. 2) (Table 3). Like as in lymphocyte DNA damage, serum visfatin levels were also significantly increased in samples withdrawn after contrast enhanced MRI compared to baseline samples and compared to samples withdrawn after non-contrast enhanced MRI (Fig. 3) (Table 3). Serum hsCRP levels were not changed over the study protocol (Table 3). None of the demographic, clinical and laboratory variables were related with clinical and MRI findings of the study population (data not shown).

Table 2
Baseline demographic and laboratory characteristics of the study population.

Age (years)	31.8 ± 16.1
Gender (female/male) n[a] (%)	20/8 (71.4/28.6)
Height (m)	1.63 ± 0.08
Weight (kg)	71.2 ± 17.7
Body mass index (kg/m²)	26.6 ± 4.9
Urea (mg/dl)	33.4 ± 11.0
Creatinine (mg/dl)	0.97 ± 0.23
Uric acid (mg/dl)	5.20 ± 1.43
Fasting glucose (mmol/l)	5.13 ± 0.47
Triglyceride (mmol/l)	2.43 ± 1.07
Total cholesterol (mmol/l)	5.82 ± 1.01
HDL[b] cholesterol (mmol/l)	1.49 ± 0.34
LDL[c] cholesterol (mmol/l)	3.21 ± 0.84
VLDL[d] cholesterol (mmol/l)	1.11 ± 0.49

Values were given as mean ± standard deviation except for gender, which was given as number (percentage).
Abbreviations: [a]*n*: number, [b]HDL: high density lipoprotein, [c]LDL: low density lipoprotein, [d]VLDL: very low density lipoprotein.

Discussion

Findings of the present study reveal for the first time in the pertinent literature that the contrast enhanced MRI is associated with increased lymphocyte DNA damage and elevated serum visfatin level.

Numerous experimental studies have been performed to elucidate the pathophysiological links between GBCAs and NSF either in rats with normal renal function [13,14] or in partially (5/6) nephrectomized rats [15,16]. Contrary to the negative findings of Grant et al. [15], GBCAs were reported to be associated with the development of NSF like lesions [13,14] supporting the clinical reports.

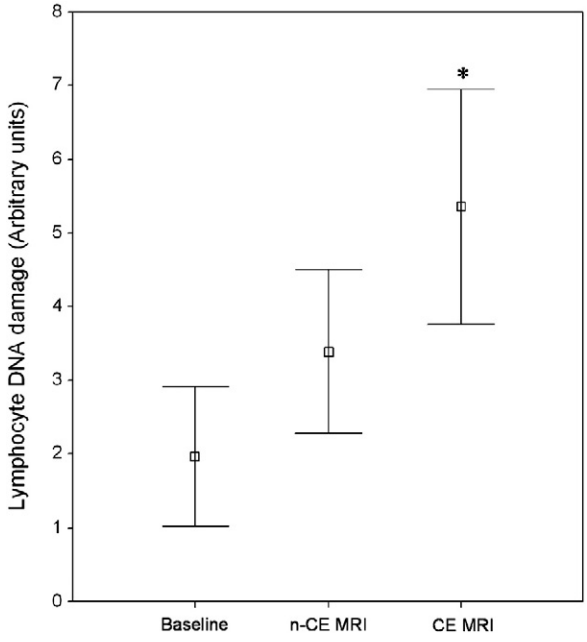

Fig. 2. Graph representing significantly increased lymphocyte DNA damage in samples withdrawn after contrast enhanced MRI compared to samples withdrawn after non-contrast enhanced MRI and compared to baseline samples. Each bars represent mean + standard error of mean (SEM). *$p<0.001$ for repeated measures of analysis of variance (ANOVA). Abbreviations: *n-CE MRI*: samples withdrawn after non-contrast enhanced magnetic resonance imaging, *CE MRI*: samples withdrawn after contrast enhanced magnetic resonance imaging.

Table 3
Lymphocyte DNA damage and serum visfatin and hsCRP levels of study population.

	Baseline	n-CE MRI[a]	CE MRI[b]	p^*
DNA damage (AU[c])	1.96 ± 2.43	3.39 ± 2.86	5.36 ± 4.12	<0.001**
Visfatin (ng/mL)	90.4 ± 19.5	102.2 ± 18.0	112.9 ± 9.5	<0.001***
hsCRP[d] (mg/dl)	0.28 ± 0.06	0.29 ± 0.05	0.27 ± 0.06	0.389

Values were given as mean ± standard deviation.
*p value for repeated measures of analysis of variance.
**p value for bivariate comparison of n-CE MRI vs. baseline: 0.079, p value for comparison of CE MRI vs. baseline samples : <0.001, p value for comparison of n-CE MRI vs. CE MRI: 0.001.
***p value for bivariate comparison of n-CE MRI vs. baseline: 0.079, p value for comparison of CE MRI vs. baseline samples : <0.001, p value for comparison of n-CE MRI vs. CE MRI: 0.011.
Abbreviations: [a]n-CE MRI: samples withdrawn after non-contrast enhanced magnetic resonance imaging, [b]CE MRI: samples withdrawn after contrast enhanced magnetic resonance imaging, [c]AU: Arbitrary units [d]hsCRP: high sensitive C - reactive protein.

Besides animal models of GBCA associated NSF, studies were performed to assess the impact of GBCA on fibroblasts/fibrocytes either in cell cultures or in rats. Omniscan® stimulated proliferation of normal human skin fibroblasts in culture [17] both at high (10–500 μmol/L) and at low (0.5–25 μmol/L) concentrations [18]. Vakil et al. [19] proposed interference of Omniscan® with the regulatory action of signals that inhibit the differentiation of monocytes to fibrocytes as the mechanism of Omniscan® induced increase in fibrocytes. Beyond the influences on fibroblasts/fibrocytes GBCAs were also reported to increase hyaluronan [20,21] and in type 1 collagen [22,23] supporting old studies revealing the stimulatory role of lanthanides in fibrillogenesis [24,25]. Increase in collagen was elucidated with decreased collagenolytic activity [22,23] which is chiefly controlled with GBCA induced changes in matrix metalloproteinases [18,20,22,23], as much greater increase in tissue inhibitor of metalloproteinase (TIMP)-1 compared to matrix metalloproteinase (MMP)-1 leads to unopposed TIMP-1 effect to increase collagen deposition [22].

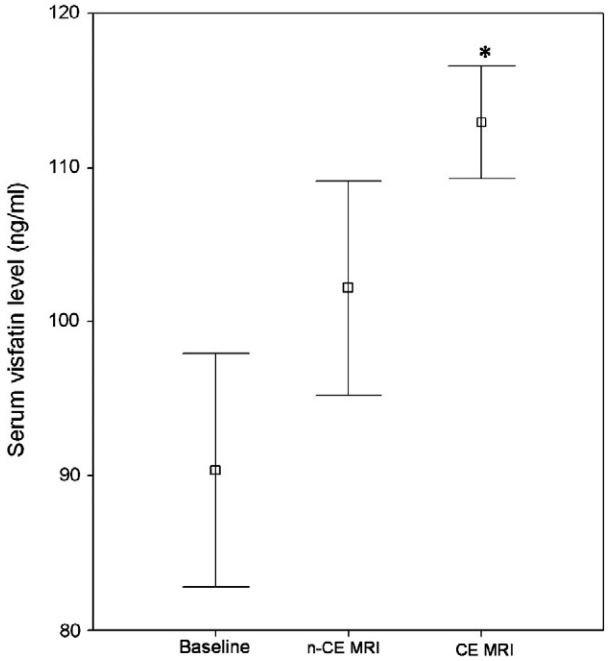

Fig. 3. Graph representing significantly increased serum visfatin level in samples withdrawn after contrast enhanced MRI compared to samples withdrawn after non-contrast enhanced MRI and compared to baseline samples. Each bars represent mean ± standard error of mean (SEM). *p<0.001 for repeated measures of analysis of variance (ANOVA). Abbreviations: *n-CE MRI*: samples withdrawn after non-contrast enhanced magnetic resonance imaging, *CE MRI*: samples withdrawn after contrast enhanced magnetic resonance imaging.

Visfatin was established to promote proliferation of rat cardiac fibroblasts and collagen synthesis which indicates that visfatin might play a role in myocardial fibrosis [26], whereas increased lymphocyte DNA damage was reported in chronic fibroproliferative disorders like systemic sclerosis [27], rheumatoid arthritis [28], and chronic inflammatory liver diseases [29]. Consequently, both increased lymphocyte DNA damage and increased serum visfatin level might play crucial role in GBCA induced NSF/NSF like lesions by favoring profibrotic/fibrotic cascade. Reports revealing increased lymphocyte DNA damage [30] and increased serum visfatin level [31] in renal failure might also suggest the role of lymphocyte DNA damage and visfatin in contrast enhanced MRI induced NSF development in case of renal dysfunction.

In cytokine based studies on NSF; Wermuth et al. [32] reported stimulatory effect of chelated and unchelated gadolinium on circulating monocytes to increase proinflammatory and profibrotic cytokines like vascular endothelial growth factor (VEGF), interleukin-13, interleukin-4, interleukin-6, transforming growth factor-β, interferon-γ in cell culture, whereas Steger-Hartmann et al. [33] revealed gadodiamide induced increase in serum levels of VEGF, osteopontin and TIMP-1 in rats. DNA damage was shown to induce production of interleukin-6, interleukin-8 [34], whereas visfatin was reported to trigger increased production of interleukin-1, interleukin-6 and tumor necrosis factor-α [11], VEGF, MMP-2/9 [35]. Accordingly triggering cytokine induction might be a plausible pathophysiological mechanism linking either increased lymphocyte DNA damage or increased serum visfatin level with contrast enhanced MRI induced NSF development.

This study further signifies visfatin rather than hsCRP as a considerable and rapidly evolving proinflammatory cytokine after contrast enhanced MRI. Defining visfatin as proinflammatory adipokine and defining hsCRP as the surrogate marker of inflammation might be the basis of the divergent findings with regard to levels of visfatin and hsCRP in the present study since increase in serum hsCRP level is mainly induced by cytokines like interleukin-6, interleukin-1 and tumor necrosis factor [36] which are activated by visfatin [11]. Unchanged serum hsCRP levels in contrast to increased serum visfatin level after contrast enhanced MRI in the present study might be explained with absence of late follow-up blood samples.

Several limitations of the present study should be considered. First of all study population was fairly limited. As a second limitation alkaline comet assay is a semiquantitative method although alkaline comet assay was originally developed to measure DNA strand breaks with high sensitivity [37]. As a third limitation claustrophobia might have influenced both lymphocyte DNA damage and serum visfatin level in the present study although the present study was neither planned nor has power to discriminate the possible influence of claustrophobia. Additionally, findings of the present study with omniscan® cannot be generalized to other GBCAs as their effect (s) on lymphocyte DNA damage, serum levels of hsCRP and visfatin remains to be evaluated.

As a conclusion, the present study reveals increased lymphocyte DNA damage and increased serum visfatin level after contrast enhanced MRI. Further animal and cell culture studies assessing the pathophysiological basis of the association between contrast enhanced MRI and increased lymphocyte DNA damage and increased serum visfatin level would enrich the findings of the present study.

References

[1] Cowper SE, Robin HS, Steinberg SM, Su LD, Gupta S, LeBoit PE. Scleromyxedema-like cutaneous diseases in renal-dialysis patients. Lancet 2000;356:1000–1.
[2] Swartz RD, Crofford LJ, Phan SH, Ike RW, Su LD. Nephrogenic fibrosing dermopathy: a novel cutaneous fibrosing disorder in patients with renal failure. Am J Med 2003;114:563–72.

[3] Mcneill AM, Barr RJ. Scleromyxedema-like fibromucinosis in a patient undergoing hemodialysis. Int J Dermatol 2002;41:364–7.
[4] Neudecker BA, Stern R, Mark LA, Steinberg S. Scleromyxedema-like lesions of patients in renal failure contain hyaluronan: a possible pathophysiological mechanism. J Cutan Pathol 2005;32:612–5.
[5] Mendoza FA, Artlett CM, Sandorfi N, Latinis K, Piera-Velazquez S, Jimenez SA. Description of 12 cases of nephrogenic fibrosing dermopathy and review of the literature. Semin Arthritis Rheum 2006;35:238–49.
[6] Morcos SK, Haylor J. Pathophysiology of nephrogenic systemic fibrosis: a review of experimental data. World J Radiol 2010;2:427–33.
[7] Grobner T. Gadolinium—a specific trigger for the development of nephrogenic fibrosing dermopathy and nephrogenic systemic fibrosis? Nephrol Dial Transplant 2006;21:1104–8.
[8] Marckmann P, Skov L, Rossen K, Dupont A, Damholt MB, Heaf JG, et al. Nephrogenic systemic fibrosis: suspected causative role of gadodiamide used for contrast-enhanced magnetic resonance imaging. J Am Soc Nephrol 2006;17: 2359–62.
[9] Möller P, Knudsen LE, Loft S, Wallin H. The comet assay as a rapid test in biomonitoring occupational exposure to DNA-damaging agents and effect of confounding factors. Cancer Epidemiol Biomarkers Prev 2000;9:1005–15.
[10] Samal B, Sun Y, Stearns G, Xie C, Suggs S, McNiece I. Cloning and characterization of the cDNA encoding a novel human pre-B-cell colony-enhancing factor. Mol Cell Biol 1994;14:1431–7.
[11] Moschen AR, Kaser A, Enrich B, Mosheimer B, Theurl M, Niederegger H, et al. Visfatin, an adipocytokine with proinflammatory and immunomodulating properties. J Immunol 2007;178:1748–58.
[12] Singh NP, McCoy MT, Tice RR, Schneider EL. A simple technique for quantitation of low levels of DNA damage in individual cells. Exp Cell Res 1988;175:184–91.
[13] Sieber MA, Pietsch H, Walter J, Haider W, Frenzel T, Weinmann HJ. A preclinical study to investigate the development of nephrogenic systemic fibrosis: a possible role for gadolinium-based contrast media. Invest Radiol 2008;43:65–75.
[14] Sieber MA, Lengsfeld P, Walter J, Schirmer H, Frenzel T, Siegmund F, et al. Gadolinium-based contrast agents and their potential role in the pathogenesis of nephrogenic systemic fibrosis: the role of excess ligand. J Magn Reson Imaging 2008;27:955–62.
[15] Grant D, Johnsen H, Juelsrud A, Løvhaug D. Effects of gadolinium contrast agents in naïve and nephrectomized rats: relevance to nephrogenic systemic fibrosis. Acta Radiol 2009;50:156–69.
[16] Pietsch H, Lengsfeld P, Steger-Hartmann T, Lowe A, Frenzel T, Hütter J, et al. Impact of renal impairment on long-term retention of gadolinium in the rodent skin following the administration of gadolinium-based contrast agents. Invest Radiol 2009;44:226–33.
[17] Edward M, Quinn JA, Mukherjee S, Jensen MB, Jardine AG, Mark PB, et al. Gadodiamide contrast agent 'activates' fibroblasts: a possible cause of nephrogenic systemic fibrosis. J Pathol 2008;214:584–93.
[18] Varani J, DaSilva M, Warner RL, Deming MO, Barron AG, Johnson KJ, et al. Effects of gadolinium-based magnetic resonance imaging contrast agents on human skin in organ culture and human skin fibroblasts. Invest Radiol 2009;44:74–81.
[19] Vakil V, Sung JJ, Piecychna M, Crawford JR, Kuo P, Abu-Alfa AK, et al. Gadolinium-containing magnetic resonance image contrast agent promotes fibrocyte differentiation. J Magn Reson Imaging 2009;30:1284–8.
[20] DaSilva M, O'Brien Deming M, Fligiel SE, Dame MK, Johnson KJ, Swartz RD, et al. Responses of human skin in organ culture and human skin fibroblasts to a gadolinium-based MRI contrast agent: comparison of skin from patients with end-stage renal disease and skin from healthy subjects. Invest Radiol 2010;45:733–9.
[21] Edward M, Quinn JA, Burden AD, Newton BB, Jardine AG. Effect of different classes of gadolinium-based contrast agents on control and nephrogenic systemic fibrosis-derived fibroblast proliferation. Radiology 2010;256:735–43.
[22] Perone PA, Weber SL, DaSilva M, Paruchuri T, Bhagavathula N, Aslam MN, et al. Collagenolytic activity is suppressed in organ-cultured human skin exposed to a gadolinium-based MRI contrast agent. Invest Radiol 2010;45:42–8.
[23] Bhagavathula N, DaSilva M, Aslam MN, Dame MK, Warner RL, Xu Y, et al. Regulation of collagen turnover in human skin fibroblasts exposed to a gadolinium-based contrast agent. Invest Radiol 2009;44:433–9.
[24] Evans CH, Drouven BJ. The promotion of collagen polymerization by lanthanide and calcium ions. Biochem J 1983;213:751–8.
[25] Drouven BJ, Evans CH. Collagen fibrillogenesis in the presence of lanthanides. J Biol Chem 1986;261:11792–7.
[26] Yu XY, Qiao SB, Guan HS, Liu SW, Meng XM. Effects of visfatin on proliferation and collagen synthesis in rat cardiac fibroblasts. Horm Metab Res 2010;42:507–13.
[27] Avouac J, Borderie D, Ekindjian OG, Kahan A, Allanore Y. High DNA oxidative damage in systemic sclerosis. J Rheumatol 2010;37:2540–7.
[28] Altindag O, Karakoc M, Kocyigit A, Celik H, Soran N. Increased DNA damage and oxidative stress in patients with rheumatoid arthritis. Clin Biochem 2007;40: 167–71.
[29] Shimoda R, Nagashima M, Sakamoto M, Yamaguchi N, Hirohashi S, Yokota J, et al. Increased formation of oxidative DNA damage, 8-hydroxydeoxyguanosine, in human livers with chronic hepatitis. Cancer Res 1994;54:3171–2.
[30] Stoyanova E, Sandoval SB, Zúñiga LA, El-Yamani N, Coll E, Pastor S, et al. Oxidative DNA damage in chronic renal failure patients. Nephrol Dial Transplant 2010;25: 879–85.
[31] Axelsson J, Witasp A, Carrero JJ, Qureshi AR, Suliman ME, Heimbürger O, et al. Circulating levels of visfatin/pre-B-cell colony-enhancing factor 1 in relation to genotype, GFR, body composition, and survival in patients with CKD. Am J Kidney Dis 2007;49:237–44.
[32] Wermuth PJ, Del Galdo F, Jiménez SA. Induction of the expression of profibrotic cytokines and growth factors in normal human peripheral blood monocytes by gadolinium contrast agents. Arthritis Rheum 2009;60:1508–18.
[33] Steger-Hartmann T, Raschke M, Riefke B, Pietsch H, Sieber MA, Walter J. The involvement of pro-inflammatory cytokines in nephrogenic systemic fibrosis—a mechanistic hypothesis based on preclinical results from a rat model treated with gadodiamide. Exp Toxicol Pathol 2009;61:537–52.
[34] Rodier F, Coppé JP, Patil CK, Hoeijmakers WA, Muñoz DP, Raza SR, et al. Persistent DNA damage signaling triggers senescence-associated inflammatory cytokine secretion. Nat Cell Biol 2009;11:973–9.
[35] Adya R, Tan BK, Punn A, Chen J, Randeva HS. Visfatin induces human endothelial VEGF and MMP-2/9 production via MAPK and PI3K/Akt signalling pathways: novel insights into visfatin-induced angiogenesis. Cardiovasc Res 2008;78:356–65.
[36] Jialal I, Devaraj S, Venugopal SK. C-reactive protein: risk marker or mediator in atherothrombosis? Hypertension 2004;44:6–11.
[37] Collins AR. Oxidative DNA damage, antioxidants, and cancer. Bioessays 1999;21: 238–46.